Clinical Investigation

Non-Gadolinium-Enhanced 3-Dimensional Magnetic Resonance Angiography

for the Evaluation of Thoracic Aortic Disease: A Preliminary Experience

Monvadi B. Srichai, MD, FACC
Sooah Kim, MD
Leon Axel, MD, PhD
James Babb, PhD
Elizabeth M. Hecht, MD

We compared image quality and diagnostic accuracy of a noncontrast 3-dimensional magnetic resonance angiography (NC-MRA) technique (balanced steady-state free-precession sequence) to contrast-enhanced MRA (CE-MRA) for evaluation of thoracic aortic disease.

The CE-MRA provides 3-dimensional high-resolution images of the thoracic aorta that are important in the evaluation of patients with aortic disease. However, recent concerns with the potential nephrotoxic effects of gadolinium contrast medium limit the application of CE-MRA for patients who have significant renal insufficiency.

Twenty-one patients (mean age, 51 yr; 18 men) who underwent NC-MRA and CE-MRA for evaluation of thoracic aortic disease were retrospectively identified. Data sets were reviewed by 2 readers who were blinded to the patients' information. The thoracic aorta was divided into 5 segments. Image quality and reader confidence for diagnosis of aortic pathology were rated on 5-point scales. The Wilcoxon matched-pairs signed rank test and the Student t test were used for comparisons.

The NC-MRA identified all pathologic findings with 100% diagnostic accuracy and similar reader confidence, when compared with CE-MRA. Although overall image quality was not significantly different, superior image quality was observed at the aortic root (4.4 ± 0.8 vs 3.2 ± 0.9, $P < 0.0005$) and ascending aorta (4.1 ± 1 vs 3.7 ± 0.9, $P = 0.05$) respectively.

In conclusion, NC-MRA is a useful alternative for evaluation and follow-up of thoracic aortic disease, especially for patients with poor intravenous access or contraindications to gadolinium use. ***(Tex Heart Inst J 2010;37(1):58-65)***

Key words: *Aneurysm, dissecting/diagnosis; aorta, thoracic/pathology; aortic aneurysm, thoracic/diagnosis; aortic diseases/diagnosis/radiography; artifacts; contrast media/toxicity; gadolinium/diagnostic use/toxicity; magnetic resonance angiography; retrospective studies*

From: *Department of Radiology, New York University School of Medicine, New York, New York 10016*

Address for reprints: *Monvadi B. Srichai, MD, FACC, Department of Radiology, New York University School of Medicine, 530 First Ave., HCC-C48, New York, NY 10016*

E-mail: *srichm01@med.nyu.edu*

Contrast-enhanced magnetic resonance angiography (CE-MRA) is often used for initial assessment and follow-up of thoracic aortic disease.[1,2] Fast, reproducible, 3-dimensional (3-D) high-resolution imaging of the thoracic aorta is essential for surgical planning and follow-up after intervention. Although computed tomographic angiography has advanced rapidly over the past few years and now can provide high-resolution images of the thoracic aorta, it has several drawbacks, including its use of ionizing radiation and nephrotoxic iodinated contrast agents and its inability to quantify blood flow. Contrast-enhanced MRA has such limitations as its need for intravenous gadolinium-chelate contrast, its frequent application without cardiac gating (which leads to motion artifacts), and its predominantly intraluminal imaging of the aorta[3] (with restricted imaging of the aortic wall for the evaluation of mural and extraluminal disease such as intramural hematoma or vasculitis). Gadolinium-chelate contrast agents are far less likely to elicit allergic-type reactions than are iodinated contrast agents, and are, in general, considered safer for use in patients with impaired renal function. Recently, however, they have been associated with nephrogenic systemic fibrosis, a potentially life-threatening disease that chiefly affects patients on dialysis or with severe renal dysfunction.[4,5]

Electrocardiographic (ECG) gated 2-dimensional noncontrast imaging techniques, including spin-echo, gradient-echo, and time-of-flight pulse sequences, enable improved visualization of the aorta without need for contrast but are hampered by longer imaging times and nonvolumetric data acquisition.[6] Recently, a respiratory- and cardiac-gated, fat-suppressed, noncontrast 3-D magnetic resonance angiography (NC-MRA) technique (balanced steady-state free-precession sequence) has been developed for whole-heart imaging,[7,8] and this provides high and isotropic spatial resolution for the evaluation of coronary arteries.[9,10] It is unknown whether this technique

can be applied to the imaging of various aortic diseases with reliable diagnostic accuracy, although recent preliminary results are promising.[11-13] The aim of this study was to examine our institution's initial experience in comparing the image quality and diagnostic accuracy of NC-MRA to those of CE-MRA for the evaluation of the anatomy and pathology of the thoracic aorta and branch vessels.

Patients and Methods

Our study was approved by the institutional review board at our medical center and was found to comply with the Health Insurance Portability and Accountability Act. The need for informed consent was waived. Given our prior experience with NC-MRA for the evaluation of coronary artery disease, as of February 2007, a modified version of this sequence was incorporated into our department's MAGNETOM Avanto 1.5T (Siemens AG; Erlangen, Germany) thoracic aorta MRA protocol. Retrospective review of our imaging database identified 21 patients (mean age, 51 yr; 18 men) who had undergone evaluation for thoracic aortic disease from February through June 2007 by means of NC-MRA, followed by CE-MRA during the same examination. Patients had been referred for evaluation of suspected aortic aneurysm (n=6), congenital vascular disease (n=8), known dissection (n=2), vasculitis (n=1), and atheromatous disease (n=4). No patient was excluded due to poor image quality.

Magnetic Resonance Technique

All patients included in this study underwent ECG- and respiratory-gated NC-MRA and routine nongated CE-MRA in the same session; these examinations were performed using a 6-channel phased-array coil combined with an 8-element spine coil. Depending on the suspected disease process, 3-D imaging was performed in either the coronal plane (for the evaluation of congenital vascular disease or vasculitis) or the oblique sagittal plane (for primary aortic disease). Noncontrast-MRA was performed using an ECG-gated and respiratory-triggered 3-D balanced steady-state free-precession sequence with T_2 preparation and fat suppression. Image acquisition was set to occur during mid-to-late diastole of the cardiac cycle. Respiratory gating was accomplished by placing cross-excitation pencil-beam navigator pulses at the dome of the liver and by using an acceptance window of ±3 mm. Imaging parameters were repetition time, 3.7 ms; trigger delay, 400 ms; echo time, 1.4 to 1.8 ms; flip angle, 90°; generalized autocalibrating partially parallel acquisitions (GRAPPA) acceleration factor, 2; mean voxel size, 1.6 × 1.7 × 2.6 mm (0.9 × 0.9 × 1.4 mm with interpolation); mean acquisition time, 9 min 9 sec ± 4 min 1 sec (range, 3 min 9 sec–20 min 51 sec; median time, 9 min 21 sec), and navigator efficiency rate, 23% to 69% (median, 50%). On the basis of our early evaluations, which demonstrated poor signals at the level of great-vessel origins, local magnetic-field shimming at the level of the great-vessel origins was performed in the last 6 of the 21 patients in this study. Contrast-enhanced MRA was always performed after the NC-MRA using a 3-D spoiled gradient-echo sequence with the following parameters: repetition time, 3.2 to 3.4 ms; echo time, 1.1 to 1.3 ms, GRAPPA acceleration factor, 2; mean voxel size, 1 × 0.9 × 1.3 mm (no interpolation was used); average time of acquisition, 17 ± 2.5 sec (range, 12.8–21.8 sec) before and after injection of Magnevist® 0.1 mmol/kg Gd-diethylenetriamine penta-acetic acid (Bayer Healthcare Pharmaceuticals Inc.; Wayne, NJ) at 2 mL/sec via a power injector (Medrad, Inc. USA; Warrendale, Pa) after a scan delay determined by test-bolus injection of 1 mL of total weight-based dose of contrast medium and a timing formula.

Image Analysis

Data sets were independently interpreted by 2 readers (MBS and EH) with 5 years' experience each, who had been blinded to patient information and prior results and who used a 3-D workstation (Multimodality Workplace, Siemens Medical Solutions). Although the readers could not be blinded to which sequence was under interpretation (NC-MRA vs CE-MRA), they read data sets in random order, with a delay of at least 2 weeks between assessments of the same patient's images, to reduce interpretation bias. For CE-MRA, the unsubtracted raw data sets were used for all analyses.

The following parameters were assessed by both readers:

Image quality was rated on a 5-point scale (1 = uninterpretable, 2 = poor, 3 = satisfactory, 4 = good, 5 = excellent) on the basis of visualization of the lumen, aortic wall, branch vessel (or coronary artery) origins, and artifacts. The image quality of predefined aortic segments (the root, ascending, arch, and descending segments, and the great-vessel origins) was determined (Fig. 1), and the mean image-quality score was calculated for the entire thoracic aorta. The root encompassed the region from the aortic annulus to the sinotubular junction. The ascending aorta encompassed the region from the sinotubular junction to the takeoff of the 1st great vessel (usually the right brachiocephalic artery). The arch encompassed the region between the 1st great-vessel takeoff and the ductus bump. The descending aorta encompassed the region from the ductus bump to the diaphragm. The arch vessels were evaluated for a distance of at least 6 cm distal to their origin.

Luminal diameters and areas of the aorta were measured from inner wall to inner wall at predefined levels (Fig. 1), including the normal-diameter values from echocardiography[14] (within parentheses): the aortic root,

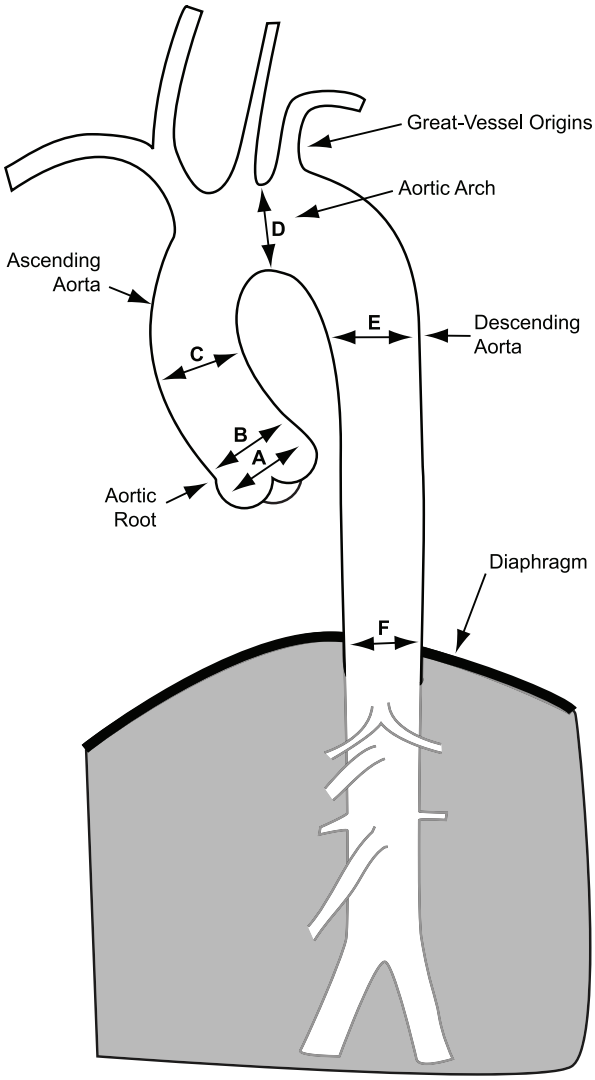

Fig. 1 *This diagram of the thoracic aorta demonstrates the segments used for the evaluation of image quality and the levels used for the measurement of aortic dimensions, including the sinus of Valsalva (A), sinotubular junction (B), mid-ascending aorta (C), mid-aortic arch (D), mid-descending aorta (E), and diaphragm level (F).*

including measurements at the aortic sinuses (<37 mm) and the sinotubular junction (<37 mm); the ascending aorta at the level of the pulmonary bifurcation (<39 mm); the aortic arch between the left common carotid and left subclavian artery takeoffs (<35 mm); the descending aorta at the level of the pulmonary bifurcation (<28 mm); and the descending aorta at the diaphragmatic level (<28 mm).

Recognition of relevant aortic diseases was noted, with readers' confidence in the diagnosis scored on a 5-point ordinal scale: 1 = uninterpretable, 2 = poorly identified with uncertain diagnosis, 3 = identified with probable diagnosis, 4 = clearly identified with highly probable diagnosis, 5 = very clearly identified with definite diagnosis. In particular, specific note was made of the presence or absence of aortic aneurysm; classic aortic dissection and communication sites; intramural hematoma; aortic coarctation; and severe (>4-mm thick) or complex aortic atheroma.

In addition to evaluating NC-MRA and CE-MRA data sets, our readers evaluated each patient's entire aortic examination at a separate session for the identification of relevant aortic disease, and this was used as the reference standard. Moreover, the location, severity (largest or narrowest diameter), and extent of the disease were recorded.

Statistical Analysis

All variables are expressed as mean ± SD. Comparisons between the 2 techniques for continuous variables were made by the paired Student *t* test. Comparisons between the 2 techniques for categorical variables were made by the Wilcoxon matched-pairs signed rank test. A probability value of $P < 0.05$ was considered statistically significant. The intra-class correlation coefficient, which is similar to the Pearson correlation but also accounts for the magnitude of difference (between readers) measured in the same segment, was used to evaluate interobserver agreement for measurements of the aortic diameters. Values near +1 were considered to represent close agreement, while values <0.9 were considered to indicate relatively poor agreement.

Results

Image Quality

Although overall image quality was not significantly different between the 2 techniques (mean image-quality score, 4.2 for NC-MRA vs 4.1 for CE-MRA; $P=0.6$), significantly higher image quality was observed at the aortic root (4.4 ± 0.8 vs 3.2 ± 0.9; $P < 0.0005$) and ascending aorta (4.1 ± 1 vs 3.7 ± 0.9; $P=0.05$), for NC-MRA compared with CE-MRA. However, this was offset by significantly lower image-quality scores at great-vessel origins (3.5 ± 1.4 vs 4.6 ± 0.7; $P < 0.005$) for NC-MRA compared with CE-MRA (Figs. 2 and 3), particularly in the initial patient studies. Improvement in the visualization of great-vessel origins could be attained with the use of local magnetic-field shimming, which was implemented in the last 6 of 21 patients (Fig. 4). Both coronary artery origins were well visualized in 16 patients in the NC-MRA group and in only 1 patient in the CE-MRA group (Fig. 5).

Aortic Dimensions

There were no significant differences between the 2 techniques in the measurements of aortic dimensions at the mid-ascending, arch, mid-descending, and diaphragm levels. However, the mean luminal diameter and area measurements were significantly higher with NC-MRA than with CE-MRA at the aortic sinus (34.6 mm

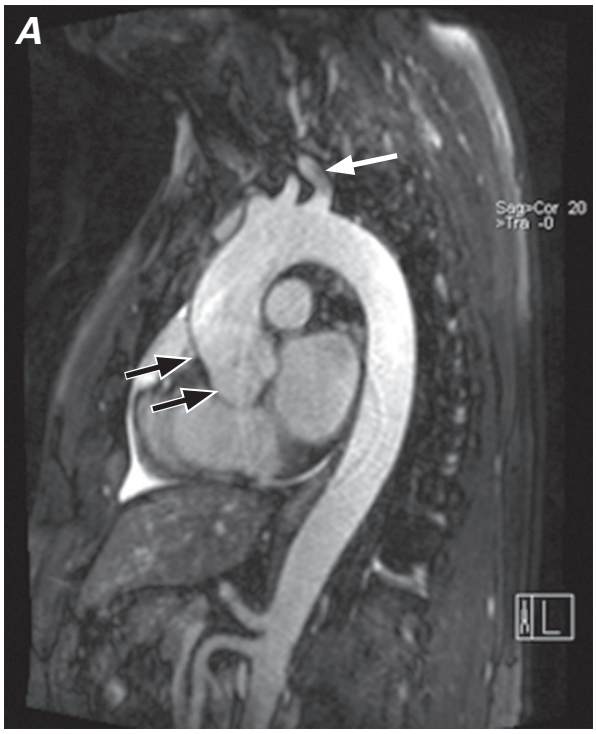

Fig. 2 *Multiplanar reformation of **A**) noncontrast magnetic resonance angiography (NC-MRA) and **B**) contrast-enhanced MRA in a patient with aneurysm of the aortic root. Image quality, particularly distinct visualization of the aortic walls, was better with NC-MRA for the aortic root and ascending aorta levels (black arrows). Magnetic-field inhomogeneities from lung parenchyma surrounding the left subclavian artery caused signal artifact in that region and consequently reduced image quality at that level (white arrow) on the NC-MRA image (top).*

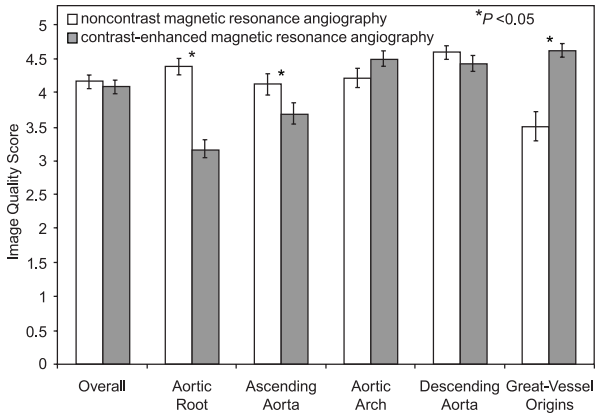

Fig. 3 *Comparison of image-quality scores between noncontrast and contrast-enhanced magnetic resonance angiography.*

vs 33.7 mm and 9.6 cm^2 vs 9.1 cm^2; $P<0.05$) and sinotubular junction (30.6 mm vs 29.7 mm and 7.5 cm^2 vs 7.1 cm^2; $P<0.01$) (Fig. 6). In addition, the intra-class correlation coefficient for NC-MRA was noted to be high (>0.9) for all aortic segments; for CE-MRA, the intra-class correlation coefficient was high (>0.9) for all aortic segments except the mid-ascending aorta.

Aortic Conditions

On the basis of imaging findings from the standard aortic protocol for all 21 subjects, there were 5 aneurysms (including 2 with dissections), 1 coarctation, 3 instances of severe or complex atheromatous disease, and 1 instance of prior coronary artery bypass grafting. These findings were all correctly diagnosed by means of both CE-MRA and NC-MRA techniques, used individually. In addition, 11 subjects without significant thoracic aortic disease were also correctly diagnosed by both CE-MRA and NC-MRA techniques, which yielded a diagnostic accuracy of 100% for each technique. For aortic dissections, an entry site could be visualized by means of both techniques. For coarctation, the smallest luminal diameter was measured at 1.2 cm by both readers. Mean reader-confidence scores were not significantly different between the 2 techniques (NC-MRA 4.17 ± 0.91 vs CE-MRA 4.26 ± 0.7, *P*=NS). No significant additional findings (for example, anomalous coronary arteries) were noted with NC-MRA in the current study.

Discussion

Contrast-enhanced MRA has become the standard imaging technique for the evaluation of thoracic aortic disease in many centers, due to its high diagnostic accuracy for intraluminal pathologic conditions such as aortic aneurysm and dissection, its fast acquisition times,[15,16] and the 3-D nature of its data sets, which is important for surgical or interventional planning.[17] However, CE-MRA techniques require intravenous access and gad-

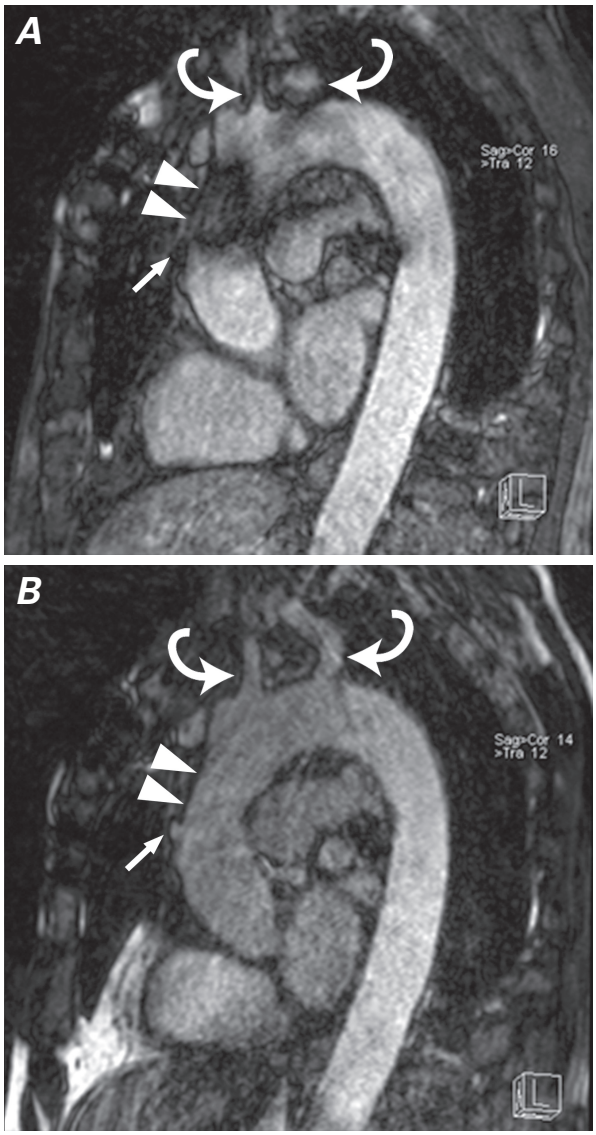

Fig. 4 *Noncontrast magnetic resonance angiography **A**) before and **B**) after localized shimming of the ascending aorta and arch in a patient with prior coronary artery bypass grafting. Before local shimming, artifact from sternal wires obscures the ascending aorta (arrowheads), and consequently the bypass graft origin (arrow). Local shimming also improves visualization of the great-vessel origins (curved arrows).*

olinium-based contrast administration, with accurate timing of contrast delivery for optimal enhancement of relevant structures.[18] In recent years, there have been increasing concerns regarding the risk of using gadolinium-based contrast agents, particularly in patients with severe renal insufficiency; therefore, alternative, nongadolinium-enhanced MRA techniques need to be reconsidered for the clinical evaluation of vascular disease.

In this study, we compared 3-D NC-MRA to conventional 3-D CE-MRA for the evaluation of thoracic aortic diseases. Although results in coronary imaging are quite promising, prior studies that used a similar technique for imaging renal arteries yielded inferior image quality when compared with CE-MRA.[19,20] For evaluation of the thoracic aorta, we found that overall image quality was not significantly different between the gated NC-MRA and CE-MRA techniques used in this study. In fact, NC-MRA provided significantly better visualization of the aortic root, ascending aorta, and coronary arteries, compared with CE-MRA. Visualization

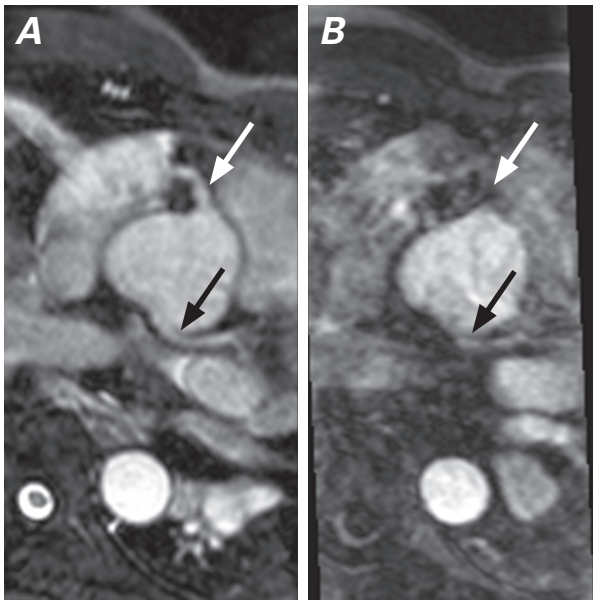

Fig. 5 ***A**) Multiplanar reformation of noncontrast magnetic resonance angiography at the level of the aortic sinuses shows good visualization of the right (white arrow) and left (black arrow) coronary arteries from their respective sinuses. **B**) Corresponding multiplanar reformation of contrast-enhanced magnetic resonance angiography at the same level shows partial visualization of the left coronary artery (black arrow) and non-visualization of the right coronary artery (white arrow).*

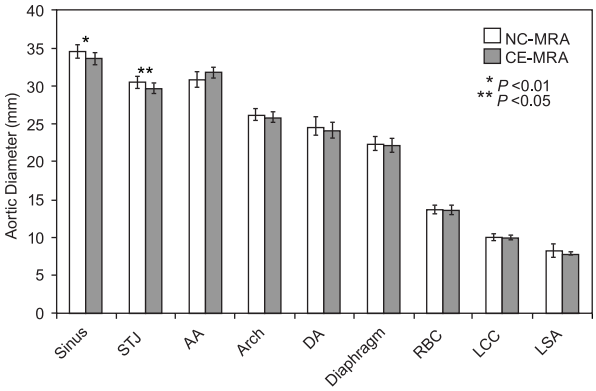

Fig. 6 *Comparison of aortic dimension measurements between noncontrast and contrast-enhanced magnetic resonance angiography.*

AA = ascending aorta; Arch = aortic arch; CE-MRA = contrast-enhanced magnetic resonance angiography; DA = descending aorta; Diaphragm = at level of diaphragm; LCC = left common carotid artery; LSA = left subclavian artery; NC-MRA = noncontrast magnetic resonance angiography; RBC = right brachiocephalic artery; Sinus = sinus of Valsalva; STJ = sinotubular junction

of these regions is important, because aortic disease can affect these regions primarily, in conjunction with other regions or independently; aortocoronary bypass grafts often originate from these regions and are also important to recognize. In addition, knowledge of the exact location and extent of disease involvement is important for preprocedural surgical planning. Image quality for the aortic root and ascending aorta were significantly worse with CE-MRA compared with NC-MRA, primarily due to cardiac motion artifact from non-ECG-gated data acquisition with CE-MRA. Although ECG-gated CE-MRA sequences are available[21,22] and are used routinely at some centers, these sequences are heart-rate dependent and often result in comparably longer imaging times with resultant requirements for longer breath-hold times and higher doses of gadolinium contrast medium.

Artifacts related to magnetic-field inhomogeneity, while present with both MRA techniques, were more prominent with NC-MRA, particularly at the left subclavian artery takeoff and, in patients with sternal wires, at the ascending aorta segment. The artifactual signal intensity loss in the great vessels is likely related to the perturbing effect of nearby lung air, which has been reported with fat-saturation sequences.[23] Although the overall image quality and the potential diagnostic performance of NC-MRA can be reduced by these artifacts, imaging with localized shimming at the aortic arch or ascending aortic segments greatly minimized artifacts in our patients (Fig. 4). As a result, we routinely used localized shimming with NC-MRA in the last 6 cases of this cohort.

There were no significant differences between the 2 sequences for measuring aortic diameters at standard anatomic landmarks, except for the aortic sinuses and sinotubular junctions. Measurements tended to be slightly higher at these levels with NC-MRA than with CE-MRA. Although no gold standard exists for measuring the aorta at these levels, it is presumed that the pulsation artifact from noncardiac-gated sequences, including CE-MRA, with the resultant blurring of the aortic walls at these levels as noted by decreased image-quality scores, may have led to inaccurate measurements with CE-MRA. Accurate measurements at these levels are important since they affect prognosis, follow-up, and future management of these patients.[24,25]

All thoracic aortic pathologic changes included in our patient cohort were recognized with use of both techniques and with similarly high diagnostic confidence scores. In particular, aortic diseases primarily affecting the aortic root and ascending aorta were more clearly depicted on NC-MRA techniques, which was likely due to the lack of ECG gating on the CE-MRA technique used in this study. Although aortic dissections could be diagnosed using both techniques, visualization of the proximal entry site and distinction between true and false lumina appeared to be more easily accomplished on CE-MRA (Fig. 7). Further evaluation of diagnostic performance of NC-MRA for the assessment of relevant structural anatomy in aortic dissections is warranted.

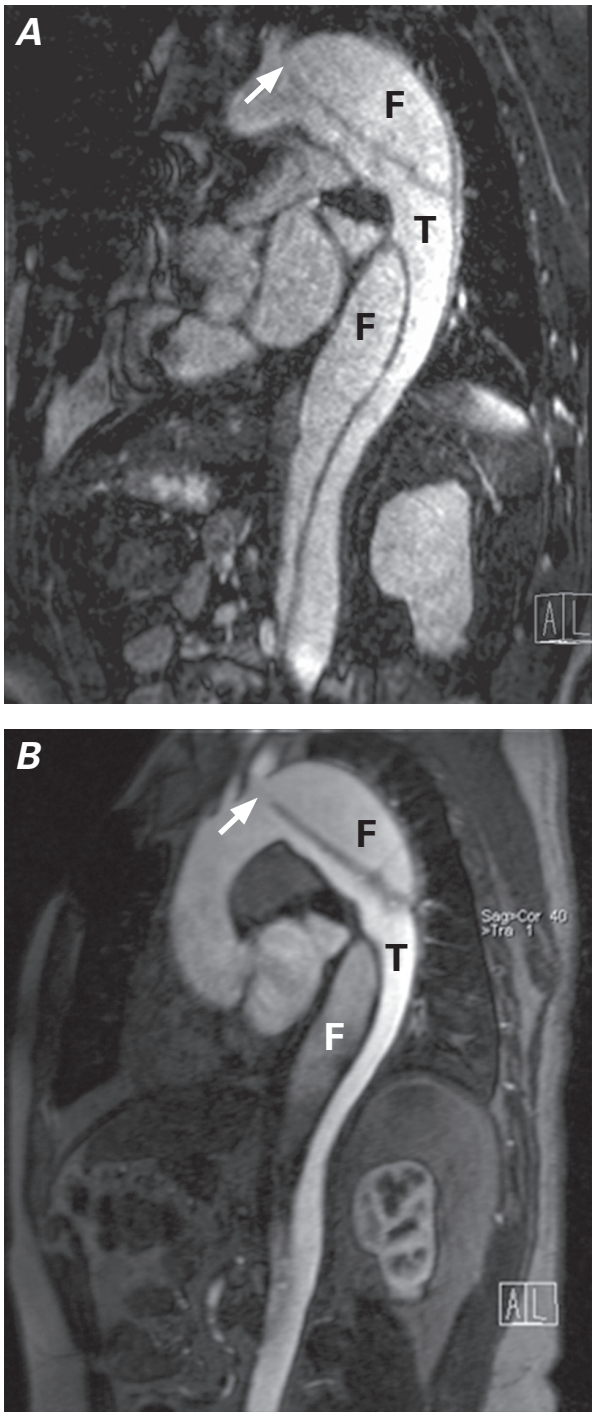

Fig. 7 *Multiplanar reformation of **A**) noncontrast and **B**) contrast-enhanced magnetic resonance angiography in a patient with type B aortic dissection. Locations of true (T) and false (F) lumina, as well as the proximal entry site (arrow), are seen with both techniques. Of note, a susceptibility artifact due to metallic sternal wires obscures the ascending aorta in the noncontrast image.*

Our findings of better visualization of the aortic root and ascending aorta with NC-MRA are similar to those of recent studies[11-13] that compared NC-MRA with gated CE-MRA, insofar as they would have been expected to provide similar image quality for these regions. However, given the different populations of patients studied in our cohort (which included patients with prior median sternotomy and aortic dissections) and given our inclusion of great-vessel anatomy in the evaluation, our study also demonstrates the inherent limitations of NC-MRA. Because prior studies[11-13] did not include evaluations of the great vessels, it is unclear whether similar decreases in image quality would have been observed in their patient populations. In our preliminary evaluation, use of local shimming techniques in the last 6 patients of our cohort appeared to reduce susceptibility to the artifact we have noted, but it is unclear whether routine local shimming would improve image quality in these regions for all patients; therefore, this warrants further study

While our study demonstrates the potential clinical usefulness of NC-MRA for the evaluation of thoracic aortic disease, it is important to note the wide range in image acquisition times (mean, 9 min 9 sec ± 4 min 1 sec; range, 3 min 9 sec–20 min 51 sec) with NC-MRA; this in general results in significantly longer imaging times, compared with CE-MRA (mean, 17 ± 2.5 sec; range, 12.8–21.8 sec). Faster image acquisition times and improvement in respiratory-gating techniques, including the use of motion-adaptive navigator pulses—along with advances in coil technology that will enable the use of higher orders of parallel imaging—can improve the efficiency of data collection and shorten overall imaging time with NC-MRA.[26] Despite the relatively long image acquisition times with NC-MRA compared with CE-MRA, it is worthwhile to consider the potential time saved overall with NC-MRA through its elimination of the need to obtain consent to administer contrast medium, to obtain intravenous access, and to determine the appropriate scan delay time (timing run).

Limitations of this study include the retrospective nature of the study design, which limits evaluation of the true diagnostic performance of each technique. Patients who had both NC-MRA and CE-MRA techniques were included. However, it is unclear if and how often technical failures may have occurred with each technique. These possible failures include the inability to complete the imaging sequence for NC-MRA consequent to difficulties with either cardiac or respiratory gating and the inability to perform CE-MRA because of inadequate intravenous access, improper timing of contrast-agent delivery, or contraindications to gadolinium-chelate contrast-agent administration (for example, pregnancy or severe renal insufficiency). Furthermore, improvements in technique and adjustments to the original protocols, such as the addition of motion-adaptive navigator pulses when available, are ongoing and can affect the overall diagnostic performance of each technique. Another limitation of this preliminary investigation is its small number of patients and its narrow variety of aortic diseases and conditions, which limits the robustness of our findings but aids in defining areas for further and more detailed investigation, such as the use of NC-MRA in the evaluation of patients with aortic dissection.

In conclusion, NC-MRA using a 3-D balanced steady-state free-precession sequence provided image quality comparable to that of CE-MRA, with 100% relative diagnostic accuracy in our study group, and provided similar diagnostic reader confidence for the recognition of important thoracic aortic disease. Further refinements in technique, such as localized shimming in regions susceptible to artifacts arising from magnetic-field inhomogeneity and use of motion-adaptive respiratory gating, may be needed to optimize image quality and improve diagnostic performance for specific cases. Although image quality may be limited in patients who have metallic implants or great-vessel disease, NC-MRA using respiratory and ECG gating is useful for screening and follow-up of thoracic aortic disease, especially in patients who have poor intravenous access, contraindications to gadolinium contrast administration (for example, pregnancy or renal failure), or inability to hold their breaths.

References

1. Krinsky GA, Rofsky NM, DeCorato DR, Weinreb JC, Earls JP, Flyer MA, et al. Thoracic aorta: comparison of gadolinium-enhanced three-dimensional MR angiography with conventional MR imaging. Radiology 1997;202(1):183-93.
2. Neimatallah MA, Ho VB, Dong Q, Williams D, Patel S, Song JH, Prince MR. Gadolinium-enhanced 3D magnetic resonance angiography of the thoracic vessels. J Magn Reson Imaging 1999;10(5):758-70.
3. Loewe C, Schillinger M, Haumer M, Loewe-Grgurin M, Lammer J, Thurnher S, et al. MRA versus DSA in the assessment of occlusive disease in the aortic arch vessels: accuracy in detecting the severity, number, and length of stenoses. J Endovasc Ther 2004;11(2):152-60.
4. Othersen JB, Maize JC, Woolson RF, Budisavljevic MN. Nephrogenic systemic fibrosis after exposure to gadolinium in patients with renal failure. Nephrol Dial Transplant 2007;22 (11):3179-85.
5. Broome DR, Girguis MS, Baron PW, Cottrell AC, Kjellin I, Kirk GA. Gadodiamide-associated nephrogenic systemic fibrosis: why radiologists should be concerned. AJR Am J Roentgenol 2007;188(2):586-92.
6. Gebker R, Gomaa O, Schnackenburg B, Rebakowski J, Fleck E, Nagel E. Comparison of different MRI techniques for the assessment of thoracic aortic pathology: 3D contrast enhanced MR angiography, turbo spin echo and balanced steady state free precession. Int J Cardiovasc Imaging 2007;23(6):747-56.
7. Shea SM, Deshpande VS, Chung YC, Li D. Three-dimensional true-FISP imaging of the coronary arteries: improved

contrast with T2-preparation. J Magn Reson Imaging 2002; 15(5):597-602.
8. Bi X, Deshpande V, Carr J, Li D. Coronary artery magnetic resonance angiography (MRA): a comparison between the whole-heart and volume-targeted methods using a T2-prepared SSFP sequence. J Cardiovasc Magn Reson 2006;8(5): 703-7.
9. Sakuma H, Ichikawa Y, Chino S, Hirano T, Makino K, Takeda K. Detection of coronary artery stenosis with whole-heart coronary magnetic resonance angiography. J Am Coll Cardiol 2006;48(10):1946-50.
10. Kim YJ, Seo JS, Choi BW, Choe KO, Jang Y, Ko YG. Feasibility and diagnostic accuracy of whole heart coronary MR angiography using free-breathing 3D balanced turbo-field-echo with SENSE and the half-fourier acquisition technique. Korean J Radiol 2006;7(4):235-42.
11. Krishnam MS, Tomasian A, Deshpande V, Tran L, Laub G, Finn JP, Ruehm SG. Noncontrast 3D steady-state free-precession magnetic resonance angiography of the whole chest using nonselective radiofrequency excitation over a large field of view: comparison with single-phase 3D contrast-enhanced magnetic resonance angiography. Invest Radiol 2008;43(6): 411-20.
12. Francois CJ, Tuite D, Deshpande V, Jerecic R, Weale P, Carr JC. Unenhanced MR angiography of the thoracic aorta: initial clinical evaluation. AJR Am J Roentgenol 2008;190(4):902-6.
13. Amano Y, Takahama K, Kumita S. Noncontrast-enhanced MR angiography of the thoracic aorta using cardiac and navigator-gated magnetization-prepared three-dimensional steady-state free precession. J Magn Reson Imaging 2008;27 (3):504-9.
14. Erbel R, Alfonso F, Boileau C, Dirsch O, Eber B, Haverich A, et al. Diagnosis and management of aortic dissection. Eur Heart J 2001;22(18):1642-81.
15. Prince MR, Narasimham DL, Jacoby WT, Williams DM, Cho KJ, Marx MV, Deeb GM. Three-dimensional gadolinium-enhanced MR angiography of the thoracic aorta. AJR Am J Roentgenol 1996;166(6):1387-97.
16. Cesare ED, Giordano AV, Cerone G, De Remigis F, Deusanio G, Masciocchi C. Comparative evaluation of TEE, conventional MRI and contrast-enhanced 3D breath-hold MRA in the post-operative follow-up of dissecting aneurysms. Int J Card Imaging 2000;16(3):135-47.
17. Farhat F, Attia C, Boussel L, Staat P, Revel D, Douek P, Villard J. Endovascular repair of the descending thoracic aorta: mid-term results and evaluation of magnetic resonance angiography. J Cardiovasc Surg (Torino) 2007;48(1):1-6.
18. Lee VS, Martin DJ, Krinsky GA, Rofsky NM. Gadolinium-enhanced MR angiography: artifacts and pitfalls. AJR Am J Roentgenol 2000;175(1):197-205.
19. Wyttenbach R, Braghetti A, Wyss M, Alerci M, Briner L, Santini P, et al. Renal artery assessment with nonenhanced steady-state free precession versus contrast-enhanced MR angiography. Radiology 2007;245(1):186-95.
20. Maki JH, Wilson GJ, Eubank WB, Glickerman DJ, Millan JA, Hoogeveen RM. Navigator-gated MR angiography of the renal arteries: a potential screening tool for renal artery stenosis. AJR Am J Roentgenol 2007;188(6):W540-6.
21. Arpasi PJ, Bis KG, Shetty AN, White RD, Simonetti OP. MR angiography of the thoracic aorta with an electrocardiographically triggered breath-hold contrast-enhanced sequence. Radiographics 2000;20(1):107-20.
22. Groves EM, Bireley W, Dill K, Carroll TJ, Carr JC. Quantitative analysis of ECG-gated high-resolution contrast-enhanced MR angiography of the thoracic aorta. AJR Am J Roentgenol 2007;188(2):522-8.
23. Axel L, Kolman L, Charafeddine R, Hwang SN, Stolpen AH. Origin of a signal intensity loss artifact in fat-saturation MR imaging. Radiology 2000;217(3):911-5.
24. Coady MA, Rizzo JA, Hammond GL, Mandapati D, Darr U, Kopf GS, Elefteriades JA. What is the appropriate size criterion for resection of thoracic aortic aneurysms? J Thorac Cardiovasc Surg 1997;113(3):476-91.
25. Coady MA, Rizzo JA, Hammond GL, Kopf GS, Elefteriades JA. Surgical intervention criteria for thoracic aortic aneurysms: a study of growth rates and complications. Ann Thorac Surg 1999;67(6):1922-6.
26. Hackenbroch M, Nehrke K, Gieseke J, Meyer C, Tiemann K, Litt H, et al. 3D motion adapted gating (3D MAG): a new navigator technique for accelerated acquisition of free breathing navigator gated 3D coronary MR-angiography. Eur Radiol 2005;15(8):1598-606.